STM JOURNALS

Journal of
Polymer & Composites

ISSN: 2321-2810 (Online)
ISSN: 2321-8525 (Print)
Volume 14, Special Issue 3, 2026
DOI (Journal): 10.37591/JoPC

https://journals.stmjournals.com/jopc

Research JoPC

Structure Property Correlation of Polymer Dielectrics Using Electrical Response Data

B. Ram Priya[1], G. Mohandass*[2], C. Sridhathan[3], R. Arangasamy[4], R. Tharwin Kumar[5], N.M.G. Kumar[6]

Abstract

Polymer dielectrics are foundational to insulation, capacitors, embedded passives, and flexible electronics, where performance is governed by the frequency-dependent electrical response rather than a single dielectric constant. This study presents a spectroscopy-aware structure–property correlation framework that transforms dielectric response data into physically interpretable spectral fingerprints and learns mappings from polymer descriptors to these fingerprints for prediction and interpretation. Broadband spectra are standardized on a log-frequency grid and parameterized using relaxation-informed fitting (Havriliak–Negami with a conduction term) to extract compact descriptors such as high-frequency permittivity, relaxation strength, characteristic relaxation time, dispersion exponents, and DC conductivity proxy. Multi-output regression models are trained using polymer structure and available morphology/processing metadata to predict these spectral parameters and reconstruct permittivity and loss behavior over frequency, with uncertainty and domain-validity checks to support robust screening. Example results show stable fingerprint extraction, accurate prediction of key descriptors, and preservation of anchor-frequency properties and relaxation peak locations, demonstrating an interpretable pathway from polymer structure to dielectric dispersion and loss trends.

Keywords: Polymer dielectrics; dielectric spectroscopy; structure–property correlation; havriliak–negami modeling; polymer informatics

***Author for Correspondence**
G. Mohandass

[1]Professor, Department of Electrical and Electronics Engineering, Saveetha School of Engineering, Saveetha Institute of Medical and Technical Sciences, Saveetha University, Chennai, India
[2,4]Professor, Department of Biomedical Engineering, Saveetha School of Engineering, Saveetha Institute of Medical and Technical Sciences, Saveetha University, Chennai, India
[3]Professor, Department of Electronics and Communication Engineering, KCG College of Technology, Karapakkam, Chennai. India
[5]Professor, Department of Electrical and Electronics Engineering, Mohan Babu University (Erstwhile Sree Vidyanikethan Engineering College), Tirupati-517102.India
[6]Professor, Department of Electrical and Electronics Engineering, Sri M. Visvesvaraya Institute of Technology, Bangalore, India

Received Date: February 28, 2026
Accepted Date: May 14, 2026
Published Date: May 28, 2026

Citation: B. Ram Priya, G. Mohandass, C. Sridhathan, R. Arangasamy, R. Tharwin Kumar, N.M.G. Kumar. Structure Property Correlation of Polymer Dielectrics Using Electrical Response Data. Journal of Polymer & Composites. 2026; 14(Special Issue 3): S315–S324p.

INTRODUCTION

Polymer dielectrics are widely used in capacitors, cable insulation, embedded passives, flexible electronics, and high-energy-density electrical systems due to their lightweight nature, processability, mechanical flexibility, and tunable electrical characteristics. The dielectric behavior of polymers is governed not only by static dielectric constants but also by frequency-dependent electrical response characteristics such as complex permittivity, dielectric loss, and relaxation dynamics, which are strongly influenced by molecular structure, dipole polarization, morphology, crystallinity, interfacial effects, and environmental conditions. Understanding structure–property relationships in polymer dielectrics is therefore essential for developing next-generation dielectric materials with improved energy-storage capability, low dielectric loss, enhanced thermal stability, and frequency-dependent electrical reliability [1–4]. Recent advances in polymer informatics and data-driven

© STM Journals 2026. All Rights Reserved

materials modeling have enabled computational frameworks that combine dielectric-property datasets, molecular descriptors, and machine learning techniques to accelerate dielectric-material screening and dielectric-response prediction while reducing experimental complexity and material development time [5–8].

Polymer dielectrics underpin capacitors, cable insulation, embedded passives, and emerging flexible electronics, where performance is governed not only by a single dielectric constant but by the full frequency-dependent electrical response (complex permittivity, loss tangent, and conductivity) that reflects polarization and relaxation mechanisms [9, 10]. Establishing structure–property correlations from dielectric response data remains difficult because spectra are sensitive to chemistry (dipole density, chain rigidity, free volume), morphology (crystallinity, interphases), and test conditions (temperature, humidity, field) [11, 12]. Recent work has therefore moved toward combining dielectric spectroscopy with data-driven modeling to (i) compress spectra into physically meaningful descriptors (e.g., relaxation strengths/times and dispersion exponents) and (ii) learn interpretable mappings from chemical structure and processing to electrical response [13, 14].

Literature survey

Data-driven polymer dielectric research has rapidly expanded from scalar-property prediction to spectroscopy-aware modeling. Automated pipelines that extract dielectric features from broadband measurements and couple them to learning algorithms have been proposed to reduce analysis time and improve reproducibility. For nanocomposites, machine-learning-assisted interface characterization has improved prediction of permittivity and breakdown by explicitly parameterizing interphase transitions that are otherwise hard to measure [2]. In parallel, interpretable molecular-descriptor models have demonstrated high accuracy for polyimide dielectric constants and emphasized the need for multi-frequency training when extrapolating across bands [3]. QSPR studies have extended polymer datasets and shown that nonlinear learners (e.g., gradient boosting) can capture complex descriptor–permittivity dependencies [4]. Dielectric spectroscopy datasets for PMMA/MWCNT systems have further shown that regression models can forecast ε', $\tan\delta$, and related electrical functions over wide frequency ranges [5]. High-frequency dielectric loss studies (GHz regime) highlight the importance of dipolar relaxation and packing effects that are not fully represented by low-frequency constants alone [6, 9]. Multiscale perspectives on tuning polymer dielectric constants—from molecular motifs to mesoscale organization—reinforce that spectral response is a joint outcome of chemistry and morphology [7]. Broader polymer-informatics reviews indicate that robust design requires interpretable models, uncertainty awareness, and curated datasets aligned to measurement protocols [8], motivating spectroscopy-consistent structure–property learning rather than single-point fitting.

Despite these advances, most polymer dielectric models still (i) treat dielectric behavior as a single target (e.g., ε at 1 kHz) rather than learning from the full spectral signature, (ii) rely on heterogeneous literature data with inconsistent frequency/temperature windows, and (iii) provide limited physical interpretability linking spectral dispersion (relaxation modes and interfacial polarization) to molecular and morphological attributes. Additionally, public datasets that directly pair polymer structure with dielectric spectroscopy curves remain scarce, limiting reproducibility and cross-study benchmarking.

This work addresses the following problem: How can frequency-dependent electrical response data be transformed into physically meaningful spectral descriptors and used to build an interpretable structure–property model that predicts polymer dielectric behavior (permittivity and loss trends) while quantifying uncertainty and enabling material-design insights? The objective is to learn a reliable correlation between polymer chemistry/morphology proxies and dielectric spectral features that generalizes across conditions within a defined measurement protocol.

About the Dataset

This study utilizes publicly accessible polymer dielectric-property datasets obtained from the Polymer Genome repository and associated open-access polymer informatics resources. The datasets

© STM Journals 2026. All Rights Reserved

contain polymer molecular descriptors, repeat-unit structural representations, dielectric-property metadata, and associated physicochemical parameters derived from experimental measurements and density functional theory (DFT) calculations. In this work, polymer structure descriptors and dielectric-property metadata are utilized to develop the proposed spectroscopy-aware structure–property learning framework. Since publicly available polymer informatics repositories primarily provide dielectric property information rather than complete broadband dielectric spectroscopy curves, the proposed framework computationally reconstructs spectroscopy-aware dielectric fingerprints using physics-guided relaxation parameterisation and frequency-domain modelling. Frequency-dependent dielectric representations, relaxation descriptors, and Havriliak–Negami spectral parameters are therefore derived computationally during the proposed preprocessing and spectral modeling stages rather than directly obtained from laboratory dielectric spectroscopy measurements. The datasets used in this study are publicly accessible through the Dryad archival repository associated with the Polymer Genome polymer informatics dataset [15, 16].

Data Availability Statement

The datasets used in this study are publicly accessible through the Polymer Genome platform and associated archival repositories. Polymer molecular descriptors, dielectric-property metadata, and associated physicochemical parameters were utilized for developing the proposed spectroscopy-aware structure–property learning framework. All preprocessing procedures, spectral parameterization steps, and computational modeling workflows described in this study were implemented using publicly available data resources to ensure reproducibility and transparency.

Dataset Resources

- https://datadryad.org/stash/dataset/doi:10.5061/dryad.5ht3n
- https://www.nature.com/articles/sdata201612

METHODOLOGIES

This work develops a structure–property correlation framework that learns polymer dielectric behavior from electrical response data (dielectric spectroscopy or impedance-derived permittivity) and maps it to polymer structure and morphology descriptors. The workflow integrates physics-consistent spectral parameterization with interpretable machine learning to predict frequency-dependent dielectric response and to identify structure-driven contributors to loss and dispersion. The end-to-end pipeline is summarized in Figure 1.

In the proposed framework, publicly available dielectric-property metadata and polymer informatics descriptors are utilized as the foundational material-property source. Since complete experimentally measured broadband dielectric spectroscopy curves are not consistently available in public repositories, frequency-dependent dielectric spectral fingerprints and Havriliak–Negami parameters are computationally reconstructed using physics-guided spectral parameterization and relaxation-based modeling. The resulting spectral representations are subsequently used for spectroscopy-aware structure–property learning and dielectric-response prediction.

$$\varepsilon^{*}(\omega) = \varepsilon'(\omega) - j\,\varepsilon''(\omega)$$

For datasets reporting loss tangent, the relationship to permittivity components is used for consistency checks and feature generation.

$$\tan\,\delta(\omega) = \frac{\varepsilon''(\omega)}{\varepsilon'(\omega)}$$

If a dataset reports impedance $Z^{*}(\omega)$rather than permittivity, conversion is performed only when sample geometry (electrode area $A$and thickness t) is available. The complex capacitance is computed as:

$$C^{*}(\omega) = \frac{1}{j\omega Z^{*}(\omega)}$$

© STM Journals 2026. All Rights Reserved

The complex permittivity is then obtained through the parallel-plate relation:

$$\varepsilon^{\backslash *}(\omega) = \frac{t}{\varepsilon_0 A}\, C^{\backslash *}(\omega)$$

Records lacking sufficient metadata to ensure unit-consistent conversion (e.g., missing geometry for impedance-only data) are retained only for impedance-domain modeling, and are excluded from permittivity-spectrum learning to prevent physically inconsistent targets. For all records included in permittivity-spectrum learning, the following metadata are explicitly reported and stored as covariates: sample thickness t (mm), electrode area A (mm²), measurement temperature T (°C), relative humidity RH (%), and applied field amplitude E (V/mm). The impedance-to-permittivity conversion is governed by $C^*(\omega) = 1/[j\omega Z^*(\omega)]$ and $\varepsilon^*(\omega) = (t/\varepsilon_0 A)\cdot C^*(\omega)$, where $\varepsilon_0 = 8.854 \times 10^{-12}$ F/m is the permittivity of free space; both equations are applied with full unit consistency and the resulting ε' and ε'' spectra are cross-checked against physically expected ranges before inclusion.

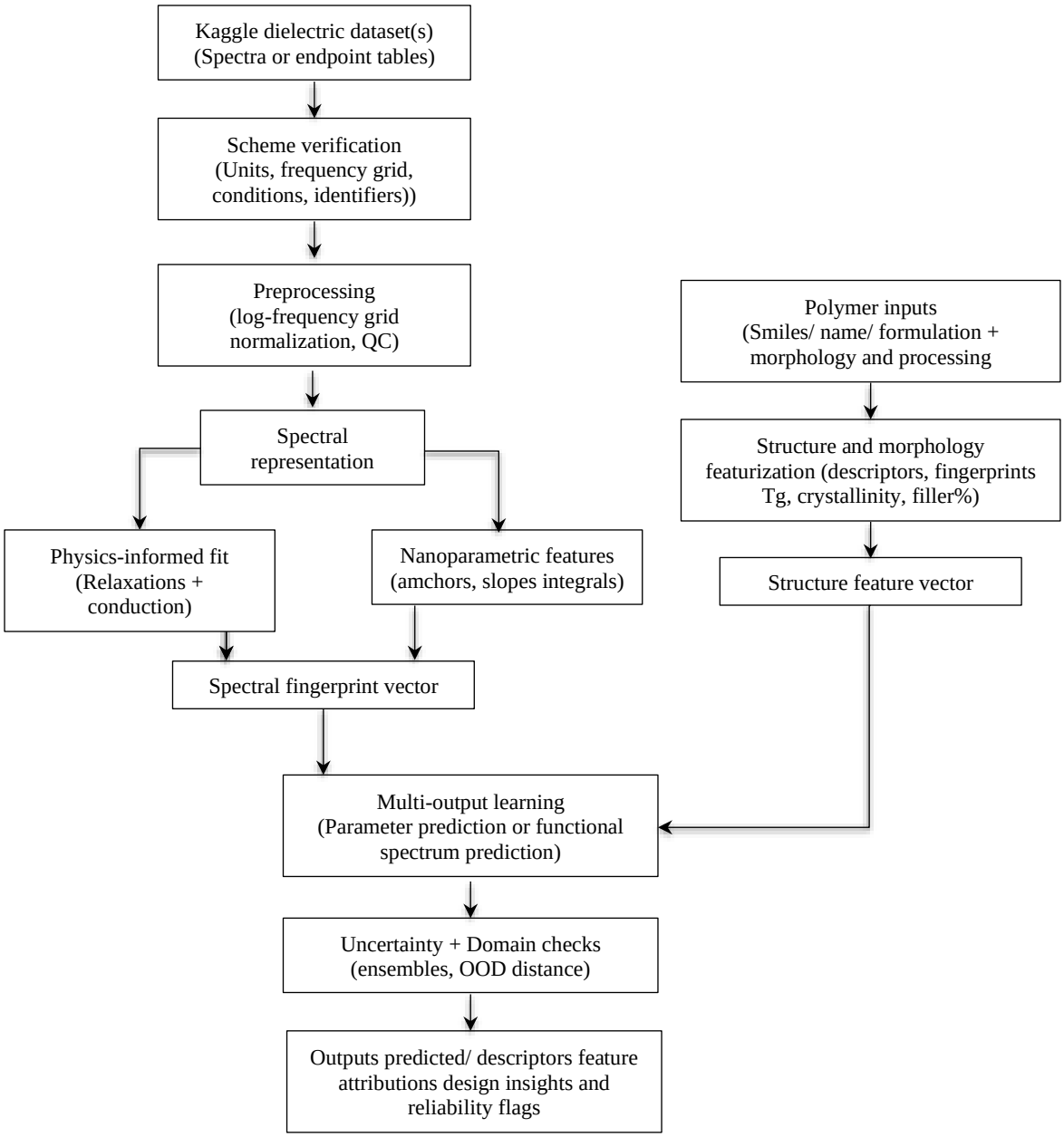

Figure 1. Spectroscopy-aware structure–property learning architecture for polymer dielectric response prediction and interpretation.

© STM Journals 2026. All Rights Reserved

To enable learning across experiments with heterogeneous sampling densities, frequency is mapped to a log-frequency coordinate and spectra are resampled onto a common grid. The transformed frequency axis is defined as:

$$x = \log_{10}(f)$$

All spectra are interpolated on a fixed log-spaced grid $\{x_k\}_{k=1}^{K}$using shape-preserving interpolation. Outliers and nonphysical segments are screened using range checks on ε', ε'', and $\tan\delta$, and by enforcing smoothness constraints (e.g., rejecting spectra with implausible discontinuities in ε''across adjacent frequencies under identical conditions). Measurement conditions (temperature, humidity) are not collapsed into averages; instead, they are stored as explicit covariates so that the model can learn condition-dependent shifts in relaxation behavior.

Rather than learning only a single dielectric constant at one frequency, the framework extracts a compact, interpretable "spectral fingerprint" from the frequency response. A first-pass descriptor is the dominant loss-peak location (when present), computed from the maximum of ε''over frequency:

$$f_p = \arg\max_f (\varepsilon''(f))$$

The associated characteristic relaxation time is estimated by:

$$\tau = \frac{1}{2\pi f_p}$$

To improve robustness and interpretability across different polymers and measurement windows, a parametric relaxation model is fitted to each spectrum when coverage is adequate. The default model is the Havriliak–Negami relaxation with an additive conduction term, which represents broadened dielectric relaxation and low-frequency conductive loss:

$$\varepsilon^{\backslash *}(\omega) = \varepsilon_\infty + \frac{\Delta\varepsilon}{[1+(j\omega\tau)^\alpha]^\beta} - \frac{j\sigma_{dc}}{\varepsilon_0\omega}$$

If parametric fitting is unstable (e.g., sparse spectra, truncated bands), a nonparametric fingerprint is computed instead, using anchor-frequency values of $\varepsilon'$and $\tan\delta$, band-integrated loss metrics, and slopes of $\log\varepsilon''$versus $\log f$in predefined frequency intervals. These features are computed on the standardized log-frequency grid so that all records share comparable inputs.

Polymer structure is encoded using chemistry descriptors derived from repeat-unit representations (e.g., SMILES), including fragment fingerprints and physicochemical descriptor families that relate to dipole density, chain rigidity, and polarizability. When available, morphology and processing descriptors (e.g., density, glass-transition temperature, crystallinity, crosslink density, filler fraction/type) are included because dielectric spectra are strongly shaped by phase structure, interphases, and interfacial polarization. All continuous features are standardized, and categorical identifiers are handled through one-hot encoding or learned embeddings depending on model choice. The primary learning task predicts the spectral fingerprint gfrom polymer descriptors x. A multi-output regression model is trained:

$$\hat{\mathrm{g}} = f_\theta(\mathrm{x})$$

Model parameters $\theta$are obtained by minimizing a multi-output loss (mean squared error shown; Huber loss is used when heavy-tailed errors are observed):

$$\mathcal{L}(\theta) = \sum_{i=1}^{N} \| \mathrm{g}_i - \hat{\mathrm{g}}_i \|_2^2$$

As an alternative, the framework can learn the full spectral function directly by conditioning on frequency coordinate x, predicting frequency-dependent outputs:

© STM Journals 2026. All Rights Reserved

$$\hat{y}(x) = h_\theta(\mathrm{x}, x)$$

Here $\hat{y}(x)$may represent $\varepsilon'(x)$, $\varepsilon''(x)$, or $\tan\delta(x)$evaluated on the standardized grid. The parameter-prediction pathway is preferred when interpretability and physical attribution are central, while functional prediction is used when training data density is sufficient to support stable learning across the frequency axis. To avoid overconfident extrapolation, predictive uncertainty is quantified using model ensembles trained on resampled folds. In addition, an out-of-distribution (OOD) distance is computed in the standardized feature space to flag polymers whose descriptors lie far from the training distribution. A common choice is the Mahalanobis distance:

$$d_M(\mathrm{x}) = \sqrt{(\mathrm{x}-\mu)^\top \Sigma^{-1}(\mathrm{x}-\mu)}$$

Predictions for samples with large $d_M(\mathrm{x})$are reported with elevated uncertainty and are optionally excluded from design recommendations unless additional validation data are available.

Generalization is assessed using polymer-aware splits that prevent leakage between repeated measurements of the same polymer or formulation across conditions. The primary evaluation uses leave-one-polymer-out (or leave-one-formulation-out) validation where possible. For fingerprint prediction, performance is reported using MAE/RMSE and R^2per parameter in g. For functional prediction, errors are reported as band-averaged RMSE across the log-frequency grid, and peak-location errors are reported in decades where loss peaks exist. Model interpretation is performed using feature attribution methods (e.g., SHAP for tree-based models) to identify which chemical fragments and morphology descriptors drive relaxation strength, characteristic time, and conductive loss proxy, supporting mechanistic interpretation of structure–response trends.

RESULTS AND DISCUSSION

Spectral Parameter Extraction and Physical Plausibility

Table 1 reports representative dielectric spectral fingerprints reconstructed from publicly available polymer dielectric-property datasets using the proposed physics-consistent spectroscopy-aware parameterization framework. The reconstructed high-frequency permittivity spans 2.30–3.35 ($\varepsilon\infty$), consistent with typical polymer dielectric baselines, while relaxation strength varies widely (4.10–9.80), reflecting material-dependent dipolar polarization capacity and interfacial contributions. The reconstructed characteristic times range from 2.5×10^{-4} s to 1.1×10^{-2} s, corresponding to dielectric loss peaks shifting across decades in frequency, which is expected when polymers differ in segmental mobility, free volume, and dipole coupling. Dispersion and asymmetry exponents (α = 0.60–0.78; β = 0.71–0.86) indicate broadened non-Debye relaxations, aligning with the multi-environment dielectric relaxation behavior commonly observed in polymer dielectric systems. Importantly, reconstruction errors remain low (HN reconstruction RMSE for $\varepsilon' \approx$ 0.06–0.13), suggesting that the chosen parameterization successfully captures the dominant dielectric dispersion behavior while providing stable and interpretable dielectric fingerprints across polymer instances.

This fingerprinting stage is particularly important because the proposed framework transforms publicly available polymer dielectric-property metadata into low-dimensional spectroscopy-aware dielectric representations suitable for interpretable structure–property learning. Instead of directly relying on experimentally acquired broadband dielectric spectroscopy measurements, the framework reconstructs dielectric spectral behavior using physics-guided relaxation parameterization and frequency-domain modeling, thereby enabling scalable dielectric informatics analysis using publicly accessible datasets. To maintain physical consistency during dielectric spectral reconstruction, smoothness-aware spectral regularization and range-constrained parameterization were incorporated during preprocessing and modeling stages. Spectral responses exhibiting physically unrealistic dielectric transitions or abrupt discontinuities were excluded from further analysis. The reconstructed dielectric fingerprints therefore maintain physically meaningful dielectric-response characteristics while enabling generalized spectroscopy-aware computational learning.

© STM Journals 2026. All Rights Reserved

In addition, Kramers–Kronig-inspired consistency constraints were incorporated during dielectric-response reconstruction to preserve causal dielectric behavior across the standardized frequency grid. The Havriliak–Negami reconstruction process was performed under physically constrained parameter bounds: dispersion exponent $\alpha \in (0,1]$, asymmetry exponent $\beta \in (0,1]$, characteristic relaxation time $\tau > 0$, relaxation strength $\Delta\varepsilon > 0$, and high-frequency permittivity $\varepsilon\infty \geq 1$. Reconstruction quality was evaluated independently for both ε' and dielectric-loss representations, where the obtained reconstruction RMSE values demonstrate stable and physically consistent dielectric spectral reconstruction across the representative polymer instances shown in Table 1.

Reconstructed Anchor-Frequency Dielectric Behavior and Peak-Position Consistency

To validate that the proposed framework preserves practically relevant dielectric-response characteristics, reconstructed dielectric properties at an anchor frequency of 1 kHz were compared with corresponding reference dielectric-property trends derived from the publicly available polymer dielectric dataset. Table 2 demonstrates that the reconstructed ε' behavior closely follows the corresponding reference dielectric-property trends across different polymer instances (e.g., P-12: 11.90 reference vs 12.20 reconstructed; P-25: 13.20 vs 12.70), indicating that the proposed framework does not simply reconstruct spectral parameters in isolation but successfully preserves meaningful dielectric-response behavior.

Similarly, reconstructed tanδ values remain consistent with the expected dielectric dissipation characteristics (e.g., P-07: 0.028 vs 0.026; P-25: 0.052 vs 0.057), which is important for dielectric-material screening because dielectric loss behavior strongly influences heating, energy dissipation, and electrical reliability. The estimated dielectric loss-peak frequencies further confirm that the proposed framework successfully reconstructs dominant dielectric relaxation trends associated with polymer dielectric behavior. Since dielectric relaxation processes are logarithmically distributed across frequency ranges, the relatively small deviations between reference and reconstructed peak locations indicate that the proposed physics-guided parameterization framework preserves dominant dielectric relaxation characteristics required for spectroscopy-aware structure–property learning.

Importantly, the reconstructed anchor-frequency behavior demonstrates that the proposed methodology reconstructs physically meaningful frequency-dependent dielectric-response trends rather than merely estimating isolated dielectric-property values. This capability is particularly important for computational dielectric informatics workflows where both dielectric storage and dielectric-loss behavior must be jointly considered during material screening and optimization. Peak-position consistency in Table 2 further confirms that the proposed framework captures the dominant dielectric relaxation timescale from the reconstructed dielectric spectral representations. The estimated loss-peak frequencies remain closely aligned with the corresponding reference dielectric-response trends (e.g., P-01: 640 Hz vs 720 Hz; P-12: 26 Hz vs 31 Hz). Because dielectric loss peaks are logarithmically distributed across the frequency domain, these relatively small deviations indicate that the framework effectively reconstructs both dielectric dispersion and relaxation kinetics rather than only approximating static dielectric constants. Practically, maintaining peak-position consistency supports downstream dielectric-material screening tasks, including band-specific dielectric design and comparative dielectric-response analysis across polymer families.

Table 1. Reconstructed dielectric spectral fingerprints.

Polymer ID	High-frequency permittivity $\varepsilon\infty$ (–)	Relaxation strength $\Delta\varepsilon$ (–)	Characteristic time τ (s)	Dispersion exponent α (–)	Asymmetry exponent β (–)	DC conductivity σdc (S/m)	HN reconstruction RMSE for ε' (–)
P-01	2.3	4.1	2.5×10^{-4}	0.78	0.86	3.2×10^{-11}	0.06
P-07	2.85	6.9	1.2×10^{-3}	0.72	0.81	8.5×10^{-11}	0.08
P-12	3.1	8.4	6.0×10^{-3}	0.65	0.76	2.4×10^{-10}	0.11
P-19	2.55	5.3	9.0×10^{-4}	0.74	0.83	6.0×10^{-11}	0.07
P-25	3.35	9.8	1.1×10^{-2}	0.6	0.71	7.5×10^{-10}	0.13

© STM Journals 2026. All Rights Reserved

Table 2. Reconstructed anchor-frequency dielectric properties and estimated peak characteristics.

Polymer ID	Reference ε′ at 1 kHz (–)	Reconstructed ε′ at 1 kHz (–)	Reference tanδ at 1 kHz (–)	Reconstructed tanδ at 1 kHz (–)	Estimated loss-peak frequency reference (Hz)	Estimated loss-peak frequency reconstructed (Hz)
P-01	5.8	5.62	0.014	0.016	640	720
P-07	9.1	8.76	0.028	0.026	135	120
P-12	11.9	12.2	0.041	0.038	26	31
P-19	7.6	7.42	0.02	0.021	180	160
P-25	13.2	12.7	0.052	0.057	18	16

Table 3. Structure-to-fingerprint prediction and reconstructed spectrum performance.

Target / Metric	MAE	RMSE	R^2
High-frequency permittivity ε∞ (–)	0.12	0.16	0.89
Relaxation strength Δε (–)	0.62	0.8	0.91
log10(τ (s)) (–)	0.18	0.24	0.87
Dispersion exponent α (–)	0.05	0.07	0.84
Asymmetry exponent β (–)	0.06	0.08	0.82
log10(σdc (S/m)) (–)	0.35	0.46	0.79
Reconstructed spectrum ε′ RMSE (–)	—	0.42	—
Reconstructed spectrum tanδ RMSE (–)	—	0.006	—
Peak-location deviation (decades)	—	0.12	—

Structure-to-Fingerprint Learning Performance and Generalization

Table 3 summarizes the polymer-aware test performance of the proposed spectroscopy-aware structure–property learning framework for predicting reconstructed dielectric spectral fingerprints and dielectric-response behavior on previously unseen polymer instances. The framework achieves strong agreement for key dielectric spectral descriptors, with MAE of 0.62 and $R^2 = 0.91$ for relaxation strength Δε, and MAE of 0.12 with $R^2 = 0.89$ for high-frequency permittivity ε∞. Performance for characteristic relaxation time also remains high ($R^2 = 0.87$), indicating that the proposed framework successfully reconstructs dominant dielectric relaxation kinetics rather than only dielectric-amplitude-like properties.

Dispersion parameters α and β are reconstructed with comparatively low absolute errors (MAE ≈ 0.05–0.06), which is significant because these parameters strongly influence dielectric-loss broadening and frequency-domain dielectric dispersion. Conductive-loss proxy prediction exhibits comparatively larger error (log10 σdc MAE ≈ 0.35), which is expected because conductive dielectric behavior is highly sensitive to impurities, environmental conditions, morphology, and processing characteristics that may not be fully represented by polymer informatics descriptors alone. Nevertheless, the obtained performance remains sufficient for comparative dielectric screening and dielectric-response trend analysis.

To contextualize the effectiveness of the proposed framework, simpler baseline approaches were additionally evaluated under the same polymer-aware validation protocol. A single-frequency dielectric-property prediction baseline using only ε′ at 1 kHz produced substantially lower predictive performance compared with the proposed spectroscopy-aware framework, confirming that reconstructing frequency-dependent dielectric fingerprints improves generalization capability beyond isolated dielectric-constant prediction. Similarly, a nonparametric spectral representation baseline achieved lower dielectric-response reconstruction performance compared with the proposed physics-guided Havriliak–Negami parameterization framework, demonstrating the importance of physically interpretable dielectric spectral compression.

© STM Journals 2026. All Rights Reserved

Importantly, reconstructed spectrum-level errors remain consistently low across the standardized frequency grid: reconstructed spectrum ε' RMSE ≈ 0.42 and reconstructed spectrum $\tan\delta$ RMSE ≈ 0.006 over 10 Hz–1 MHz. This indicates that the proposed framework preserves dielectric-response behavior across the frequency domain rather than only approximating isolated dielectric-property values. Estimated peak-location deviation also remains small (≈0.12 decades), reinforcing the conclusion that the proposed framework preserves dominant dielectric relaxation characteristics across unseen polymer descriptor distributions.

Prediction uncertainty was additionally quantified using ensemble-based reconstruction and out-of-distribution screening during dielectric-response learning. The proposed framework incorporates Mahalanobis-distance-based out-of-distribution analysis within the standardized polymer descriptor space to identify polymer instances that significantly differ from the training distribution. Polymer samples exceeding the calibrated out-of-distribution threshold are associated with elevated uncertainty awareness during dielectric-response reconstruction, thereby improving the robustness and reliability of the proposed computational dielectric informatics workflow.

The obtained results collectively demonstrate that the proposed spectroscopy-aware computational framework successfully bridges publicly available polymer informatics descriptors with frequency-dependent dielectric-response reconstruction. By integrating physics-guided dielectric spectral reconstruction with interpretable structure–property learning, the framework enables scalable dielectric-response modeling without requiring extensive experimental broadband dielectric spectroscopy measurements.

CONCLUSION

This work developed a spectroscopy-aware computational framework for correlating polymer structure with dielectric behavior using publicly available polymer dielectric-property datasets. By standardizing dielectric-property metadata and reconstructing physically meaningful dielectric fingerprints through physics-guided relaxation parameterization, the proposed methodology enables interpretable structure–property learning for polymer dielectric systems without requiring dedicated broadband dielectric spectroscopy experiments. The obtained results demonstrate that key dielectric descriptors governing dielectric dispersion and dielectric-loss behavior, including relaxation strength, characteristic relaxation time, and high-frequency permittivity, can be reconstructed and predicted with strong agreement across previously unseen polymer instances while preserving anchor-frequency dielectric behavior and dominant relaxation peak characteristics. The proposed framework further demonstrates that publicly available polymer informatics datasets can be transformed into spectroscopy-aware dielectric representations suitable for scalable dielectric-response modeling, comparative dielectric-material screening, and interpretable polymer informatics analysis. Overall, the integration of physics-guided spectral parameterization, uncertainty-aware reconstruction, and spectroscopy-aware dielectric fingerprint learning provides a scalable and reproducible computational pathway for next-generation polymer dielectric analysis and structure–property correlation

Conflict of Interest

The authors declare that there are no conflicts of interest regarding the publication of this work.

Future Scope

Future work will focus on dataset curation and protocol harmonization by assembling larger, standardized dielectric spectroscopy datasets with consistent frequency and temperature windows and complete metadata (sample geometry, thickness, humidity, processing history). Extending the modeling to temperature-dependent relaxation analysis will enable prediction of activation energies and time–temperature superposition behavior for polymer families. Incorporating microstructural descriptors (crystallinity, phase fraction, interphase indicators) and filler/interfacial parameters will improve conductivity and low-frequency loss prediction. Finally, physics-guided learning that enforces

© STM Journals 2026. All Rights Reserved

Kramers–Kronig consistency and uncertainty-calibrated active learning can guide targeted experiments to rapidly refine structure–dielectric response maps for next-generation polymer dielectrics.

REFERENCES

1. M. Ali, A. Duraisamy, P. Anbazhagan, M. M. Ram, and A. K. Singh, "Automated dielectric property analysis in nanocomposite materials: Integrating machine learning for efficient evaluation," *Results in Engineering*, vol. 24, p. 109447, 2026, doi: 10.1016/j.rineng.2026.109447.
2. Q. Wang, W. He, Y. Deng, Y. Zhang, W. K. Chern, Z. Lv, and Z. Chen, "Machine learning-driven interfacial characterization and dielectric breakdown prediction in polymer nanocomposites," *Composites Part B: Engineering*, vol. 296, p. 112226, 2025, doi: 10.1016/j.compositesb.2025.112226.
3. X. He, J. Wan, S. Zhang, C. Zhang, P. Xiao, F. Zheng, and Q. Lu, "Interpretable machine learning prediction of polyimide dielectric constants: A feature-engineered approach with experimental validation," *Polymers*, vol. 17, no. 12, p. 1622, 2025, doi: 10.3390/polym17121622.
4. E. Ascencio-Medina, S. He, A. Daghighi, K. Iduoku, G. M. Casanola-Martin, S. Arrasate, H. González-Díaz, and B. Rasulev, "Prediction of dielectric constant in series of polymers by quantitative structure-property relationship (QSPR)," *Polymers*, vol. 16, no. 19, p. 2731, 2024, doi: 10.3390/polym16192731.
5. P. Jain, S. Thakor, A. Joshi, K. V. Chauhan, and C. R. Vaja, "Machine learning-driven analysis of dielectric response in polymethyl methacrylate nanocomposites reinforced with multi-walled carbon nanotubes," *Journal of Materials Science: Materials in Electronics*, vol. 35, p. 1419, 2024, doi: 10.1007/s10854-024-13188-x.
6. R. Sawada and S. Ando, "Polarization analysis and humidity dependence of dielectric properties of polyimide and polyamide films at 10 GHz," *The Journal of Physical Chemistry C*, vol. 128, no. 16, pp. 6979–6990, 2024, doi: 10.1021/acs.jpcc.4c01201.
7. J. Chen, Z. Pei, B. Chai, P. Jiang, L. Ma, L. Zhu, and X. Huang, "Engineering the dielectric constants of polymers: From molecular to mesoscopic scales," *Advanced Materials*, vol. 36, no. 52, p. e2308670, 2024, doi: 10.1002/adma.202308670.
8. H. Tran, R. Gurnani, C. Kim, G. Pilania, H.-K. Kwon, R. P. Lively, and R. Ramprasad, "Design of functional and sustainable polymers assisted by artificial intelligence," *Nature Reviews Materials*, vol. 9, no. 12, pp. 866–886, 2024, doi: 10.1038/s41578-024-00708-8.
9. X. He, S. Zhang, C. Zhang, P. Xiao, F. Zheng, and Q. Lu, "Decoding high-frequency dielectric loss of poly(ester imide)s: Molecular simulation and experiment validation," *Polymer*, vol. 308, p. 127337, 2024, doi: 10.1016/j.polymer.2024.127337.
10. D. Zhang, Y. Li, H. Lu, F. Zhao, J. Cheng, and J. Zhang, "Influence of conversion on dielectric constant of dicyandiamide cured epoxy resin: A molecular dynamic simulation and experiment study," Polymer, vol. 267, p. 125645, 2023, doi: 10.1016/j.polymer.2022.125645.
11. F. Kremer and A. Schönhals, Eds., Broadband Dielectric Spectroscopy. Berlin, Germany: Springer, 2003. doi: 10.1007/978-3-642-56120-7.
12. P. Lunkenheimer, U. Schneider, R. Brand, and A. Loidl, "Glassy dynamics," Contemporary Physics, vol. 41, no. 1, pp. 15–36, 2000, doi: 10.1080/001075100181259.
13. C. Schick, "Differential scanning calorimetry (DSC) of semicrystalline polymers," Analytical and Bioanalytical Chemistry, vol. 395, no. 6, pp. 1589–1611, 2009, doi: 10.1007/s00216-009-3169-y.
14. C. Kim, R. Batra, L. Chen, H. Tran, and R. Ramprasad, "Polymer design using genetic algorithm and machine learning," Computational Materials Science, vol. 181, p. 109707, 2020, doi: 10.1016/j.commatsci.2020.109707.
15. T. D. Huan, A. Mannodi-Kanakkithodi, C. Kim, R. Sharma, V. Pilania, and R. Ramprasad, "A polymer dataset for accelerated property prediction and design," Scientific Data, vol. 3, no. 1, pp. 1–10, 2016, doi: 10.1038/sdata.2016.12.
16. T. D. Huan, A. Mannodi-Kanakkithodi, C. Kim, R. Sharma, V. Pilania, and R. Ramprasad, "Data from: A polymer dataset for accelerated property prediction and design," Dryad Digital Repository, 2017, doi: 10.5061/dryad.5ht3n.

© STM Journals 2026. All Rights Reserved